NeuroImage: Clinical 29 (2021) 102574

Contents lists available at ScienceDirect

NeuroImage: Clinical

journal homepage: www.elsevier.com/locate/ynicl

# Comparison of regional brain deficit patterns in common psychiatric and neurological disorders as revealed by big data

Peter Kochunov [a,*,1], Meghann C. Ryan [a], Qifan Yang [b], Kathryn S. Hatch [a], Alyssa Zhu [b], Sophia I. Thomopoulos [b], Neda Jahanshad [b], Lianne Schmaal [c,d], Paul M. Thompson [b], Shuo Chen [a], Xiaoming Du [a], Bhim M. Adhikari [a], Heather Bruce [a], Stephanie Hare [a], Eric L. Goldwaser [a], Mark D. Kvarta [a], Thomas E. Nichols [e], L. Elliot Hong [a]

[a] Maryland Psychiatric Research Center, Department of Psychiatry, University of Maryland School of Medicine, Baltimore, MD, USA
[b] Imaging Genetics Center, Stevens Neuroimaging & Informatics Institute, Keck School of Medicine of USC, Marina del Rey, CA, USA
[c] Orygen, Parkville, Australia
[d] Centre for Youth Mental Health, The University of Melbourne, Melbourne, Australia
[e] Nuffield Department of Population Health of the University of Oxford, Oxford, United Kingdom

ARTICLE INFO

*Keywords:*
Big data
Meta-analysis
DTI
Structural deficit patterns
ENIGMA
RVI

ABSTRACT

Neurological and psychiatric illnesses are associated with regional brain deficit patterns that bear unique signatures and capture illness-specific characteristics. The Regional Vulnerability Index (RVI) was developed to quantify brain similarity by comparing individual white matter microstructure, cortical gray matter thickness and subcortical gray matter structural volume measures with neuroanatomical deficit patterns derived from large-scale meta-analytic studies. We tested the specificity of the RVI approach for major depressive disorder (MDD) and Alzheimer's disease (AD) in a large epidemiological sample of UK Biobank (UKBB) participants (N = 19,393; 9138 M/10,255F; age = 64.8 ± 7.4 years). Compared to controls free of neuropsychiatric disorders, participants with MDD (N = 2,248; 805 M/1443F; age = 63.4 ± 7.4) had significantly higher RVI-MDD values ($t = 5.6$, $p = 1{\cdot}10^{-8}$), but showed no detectable difference in RVI-AD ($t = 2.0$, $p = 0.10$). Subjects with dementia (N = 7; 4 M/3F; age = 68.6 ± 8.6 years) showed significant elevation in RVI-AD ($t = 4.2$, $p = 3{\cdot}10^{-5}$) but not RVI-MDD ($t = 2.1$, $p = 0.10$) compared to controls. Even within affective illnesses, participants with bipolar disorder (N = 54) and anxiety disorder (N = 773) showed no significant elevation in whole-brain RVI-MDD. Participants with Parkinson's disease (N = 37) showed elevation in RVI-AD ($t = 2.4$, $p = 0.01$) while subjects with stroke (N = 247) showed no such elevation ($t = 1.1$, $p = 0.3$). In summary, we demonstrated elevation in RVI-MDD and RVI-AD measures in the respective illnesses with strong replicability that is relatively specific to the respective diagnoses. These neuroanatomic deviation patterns offer a useful biomarker for population-wide assessments of similarity to neuropsychiatric illnesses.

## 1. Introduction

Diagnosis of neuropsychiatric illnesses is based on meeting criteria for clinical symptoms, cognitive testing, behavioral observation, and neurological signs that may not be unique to any single illness. Many disorders show overlap: from genetic risk factors, to symptoms, to treatments, to deficit patterns. However, the disorder-oriented diagnosis system builds silos, or barriers, to understanding the degree of overlap

* Corresponding author.
*E-mail addresses:* pkochunov@som.umaryland.edu (P. Kochunov), MCRyan@som.umaryland.edu (M.C. Ryan), qifan.yang@usc.edu (Q. Yang), KHatch@som.umaryland.edu (K.S. Hatch), alyssa.zhu@ini.usc.edu (A. Zhu), sthomopo@usc.edu (S.I. Thomopoulos), neda.jahanshad@usc.edu (N. Jahanshad), lianne.schmaal@unimelb.edu.au (L. Schmaal), pthomp@usc.edu (P.M. Thompson), ShuoChen@som.umaryland.edu (S. Chen), XDu@som.umaryland.edu (X. Du), BAdhikari@som.umaryland.edu (B.M. Adhikari), HBruce@som.umaryland.edu (H. Bruce), Stephanie.Hare@som.umaryland.edu (S. Hare), EGoldwaser@som.umaryland.edu (E.L. Goldwaser), Mark.Kvarta@som.umaryland.edu (M.D. Kvarta), thomas.nichols@bdi.ox.ac.uk (T.E. Nichols), Ehong@som.umaryland.edu (L.E. Hong).
[1] PK and MR have equally contributed to this paper.

https://doi.org/10.1016/j.nicl.2021.102574
Received 23 July 2020; Received in revised form 8 December 2020; Accepted 16 January 2021
Available online 26 January 2021

and distinctions among diagnostic categories. We also lack robust brain imaging biomarkers to identify and separate among psychiatric disorders and neurological illnesses. Subject with neuropsychiatric disorders show deficits in the fractional anisotropy of white matter, cortical gray matter thickness and subcortical volume. These metrics are sensitive but not specific to any neuropsychiatric illness (Heresco-Levy et al., 2002; Hoffman et al., 2003; Kane et al., 1988; Kulkarni et al., 2015; Samara et al., 2016). Recently, epidemiological 'big data' samples have become available that include neuroimaging across many individuals including people with psychiatric and neurological illnesses. These datasets allow identification of deficit patterns that are specific to the illnesses and can help re-define their unique and shared features (Kochunov et al., 2020a, 2019b). We present findings using the Regional Vulnerability Index (RVI) to measure the similarity between an individual brain and the expected patterns derived from large scale meta-analyses using a representative psychiatric illness, major depressive disorder (MDD), and a representative neurological illness, Alzheimer's disease (AD). We further evaluate the specificity of the RVI approach in related mood and neurodegenerative illnesses.

Large and inclusive meta-analytic studies conducted by big data consortia such as the Enhancing Neuro Imaging Genetics through Meta-Analysis (ENIGMA) Consortium (Thompson et al., 2017, 2020) and Alzheimer's Disease Neuroimaging Initiative (ADNI) (Weiner et al., 2015, 2017) offer a principled way to define disease-related brain abnormalities. Several studies by ENIGMA and ADNI have reported patterns of patient-control group differences in the microstructural integrity of cerebral white matter tracts, cortical gray matter thickness and volumes of subcortical gray matter structures (Kelly et al., 2018; Kochunov et al., 2019c; Schmaal et al., 2017, 2016; van Erp et al., 2016, 2018; van Velzen et al., 2019; Zavaliangos-Petropulu et al., 2019). These deficit patterns, expressed as regional effect sizes, are highly replicable ($r$ = 0.7–0.9) and predictive of deficit patterns in independent cohorts (Kochunov and Hong, 2014; Kochunov et al., 2019a, 2016, 2019c) and cognitive impairment in people affected with these illnesses (Kochunov et al., 2020b). We proposed RVI as a simple measure of similarity between regionally derived metrics from an individual's brain MRI (e.g., regional volumes, thicknesses, microstructure measurements) and the expected pattern of those metrics with respect to the patient-control effect sizes derived from large-scale consortia.

The RVI approach assumes that the meta-analytic effect-sizes derived from such international consortia can serve as the 'ground truth' for expected disorder-specific deficit patterns. The utility of this approach was demonstrated by showing that white matter RVI for schizophrenia predicted treatment resistance in schizophrenia better than any individual imaging measure (Kochunov et al., 2019a). We later demonstrated the similarity in white matter deficit patterns across psychiatric illnesses, suggesting that RVI serves as an important index for cross-disorder research (Kochunov et al., 2020a, 2020b). However, it is unknown if the RVI approach can be extended beyond schizophrenia. We calculated an RVI for MDD and AD in a large epidemiological sample of UK Biobank (UKBB) participants (N = 19,393 with imaging data available at the time of this analysis). We evaluated the sensitivity of whole-brain RVI values and the RVIs for three types of neuroimaging measures: cortical gray matter thickness, subcortical volumes and white matter integrity; the three standard phenotypes indexed by ENIGMA workflows. The UKBB sample is composed of mainly healthy people. Approximately 10% of the sample are diagnosed with MDD but there are very few subjects with neurodegenerative disorders. Our primary aim was to evaluate the sensitivity of RVI-MDD and its specificity to other "neighboring" disorders that share mood symptoms. By using deficit patterns derived from ENIGMA (Thompson et al., 2017, 2020) and ADNI (Weiner et al., 2015, 2017) we tested the hypothesis that patterns of regional neuroanatomic deficits across neuropsychiatric illnesses - as captured by the RVI approach - are replicable and tested disease specificity.

## 2. Methods

Neuroimaging and clinical data were analyzed for a subset of N = 19,393 participants from the UK Biobank (mean age = 64.78 ± 7.44 years; 9,138 M/10,255F) for whom structural and diffusion imaging phenotypes were available. Data were collected between 2012 and 2019 in participants recruited from the United Kingdom (Manolio et al., 2012). All participants provided written informed consent. The full demographic information is available in Table 1.

### 2.1. Defining patients and controls

We used the UKBB parser software (https://github.com/USC-IGC/ukbb_parser) to identify N = 4262 subjects with ICD codes corresponding to various neuropsychiatric diagnoses. Among participants with ICD codes for psychiatric illness, we identified N = 2,248 (805 M/1443F, age = 63.4 ± 7.4) subjects with a self-reported lifetime diagnosis of MDD. N = 603 of MDD subjects also reported a comorbid diagnosis of anxiety disorder but were free from other neurological or psychiatric conditions. These subjects were kept in the analyses but post-hoc analyses were performed to test the main contrast while excluding these subjects. For psychiatric disorder comparisons, we identified subjects with mutually exclusive conditions. We identified N = 773 subjects with lifetime self-reported anxiety disorder (385/388F, age = 65.3 ± 7.2) and N = 54 with bipolar disorder (21 M/33F, age = 63.2 ± 5.7 years); who had no other reported neurological or psychiatric illnesses.

Anxiety and BD are the two of the most common mood disorders and were selected to provide a stringent control that tested how well the RVI approach can differentiate among the different mood disorders.

For neurological illnesses, we identified N = 7 subjects with Alzheimer's Disease (4 M/3F, age = 68.6 ± 8.6 years). To serve as our neurological comparison groups, we identified N = 247 individuals with stroke (150 M/97F, age = 68.9 ± 9.1 years) and N = 37 with Parkinson's Disease (24 M/14F, age = 68.7 ± 5.7 years). These subjects reported no other neurological illnesses. Parkinson's Disease and stroke were selected as neurological illness comparison groups because they are two of the most common age-related neurological disorders, and thus should provide a control to test the degree that RVI can separate neurological illnesses among those with shared clinical features.

N = 15,131 subjects (7530 M/7601F, age = 64.9 ± 7.8 years.) who were free of ICD codes corresponding to neurological or psychiatric illnesses were treated as controls.

### 2.2. Imaging protocol and processing

In this study, we examined regional cortical gray matter thickness, subcortical gray matter structural volume and tract-wise measures of FA values provided by the UKBB (see supplement). These phenotypes were extracted from neuroimaging data collected with a Siemens Skyra 3T scanner using a standard 32-channel radiofrequency (RF) head coil. The imaging protocol collected high resolution T1-weighted 3D MP-RAGE scans (resolution = 1 × 1 × 1 mm, FOV = 208 × 256 × 256,

**Table 1**
Demographic Information for UKBB sample used in this research. Controls were derived as subjects with no self-reported psychiatric or neurological illness.

| Neuropsychiatric Disorders | N Subjects (Male/Female) | Average Age ± SD |
|---|---|---|
| Major Depressive Disorder (MDD) | 2248 (805/1443) | 63.4 ± 7.4 |
| Anxiety | 773 (385/388) | 65.3 ± 7.2 |
| Bipolar Disorder (BD) | 54 (21/33) | 63.2 ± 5.7 |
| Alzheimer's Disease (AD) | 7 (4/3) | 68.6 ± 8.6 |
| Stroke | 247 (150/97) | 68.9 ± 9.1 |
| Parkinson's Disease (PD) | 37 (24/14) | 68.7 ± 5.7 |
| Controls | 15,131 (7530/7601) | 64.9 ± 7.8 |

duration = 5 min, ,sagittal, in-plane acceleration iPAT = 2, prescan-normalize) and 3D T2 FLAIR images (resolution = 1.05 × 1 × 1 mm, FOV = 192 × 256 × 256, duration = 6 min, 3D SPACE, sagittal, in-plane GRAPPA with partial phase imaging acceleration factor of 2, and partial 7/8 Fourier sampling). Diffusion data were collected with a resolution of 2 × 2 × 2 mm and two diffusion shells of $b = 1000$ and 2000 s/mm2 with 50 diffusion directions per shell and 5$b = 0$ images (FOV = 104 × 104 × 72, duration = 7 min).

Imaging data was processed using the UKBB workflow that is based on ENIGMA structural and DTI pipelines. Details of the image pre-processing and analysis are provided by UKBB (biobank.ctsu.ox.ac.uk/crystal/crystal/docs/brain_mri.pdf). Briefly, the UKBB workflow provides the measurements evaluated across many ENGIMA studies including 24 regional white matter tract FA values, 33 regional estimates of cortical GM thickness, volumes of the lateral ventricles, and 7 subcortical gray matter volumes per hemisphere that corresponded to these derived by ENIGMA workflows and (Table S1, see supplement). Measures from the left and right structures were averaged.

### 2.3. Regional deficit patterns for MDD and AD

The regional deficit patterns, represented as maps of effect sizes (Cohen's *d*-value) of patient-control deficits after correction for age and sex, were derived from samples that did not include UKBB subjects. The cortical, subcortical and white matter regional deficit patterns in MDD were derived by the ENIGMA-MDD workgroup based on their analysis of up to 20 cohorts with 40–60% cohort overlap among the studies (Schmaal et al., 2017, 2016; van Velzen et al., 2019). The MDD-DTI effect size data were taken from the Table S4 (van Velzen et al., 2019). The MDD-Cortical effect sizes were taken from the Table S5 (Schmaal et al., 2017) and averaged for both hemispheres. Subcortical effect sizes were taken from the Table S4 (Schmaal et al., 2016). All MDD effect sizes were corrected for age, sex and their interaction and site effects; subcortical effect sizes were also corrected for medications. The ADNI-AD effect sizes for DTI were taken from Table S4 (Kochunov et al., 2020b).

The white matter deficit patterns in AD were derived based on the ADNI dataset (Kochunov et al., 2020b). The cortical and subcortical deficit patterns in AD were derived using methods detailed in supplemental material (see Supplement). Briefly, the deficit patterns were derived based on the analysis of T1-weighted data for N = 898 subjects (434 M/464F, average age = 74.1 ± 6.5 years), that included N = 290 subjects with AD (159 M/131F, age = 75.12 ± 7.62 years) and 608 controls (275 M/333F, age = 73.5 ± 6.1 years) downloaded from ADNI database (ida.loni.usc.edu). All subjects available in the ADNI database were included at the time of study: ADNI1, ADNIGO/ADNI2 (ADNI2GO) and ADNI3. We excluded subjects with missing demographic information, and those that failed ENIGMA structural analysis pipeline quality control and assurance steps (http://enigma.ini.usc.edu/protocols/imaging-protocols). All AD effect sizes were corrected for age, sex and their interaction and site effects.

### 2.4. Statistics

#### 2.4.1. Regional vulnerability index

The ENIGMA consortium provided the meta-analytical ranks of the severity of regional deficits in gray matter thickness (33 cortical areas), subcortical volumes (8 structures) and fractional anisotropy (24 major white matter regions) in MDD compared to controls. These findings are presented as the MDD regional meta-analytical effect sizes reported as the Cohen's *d* statistics after adjusting for age and sex (Table S1). Calculations for the tissue specific RVIs in UKBB subjects are as follows (using FA and MDD as an example): mean FA measures for each of the 24 major white matter regions were first converted to *z* values by (1) calculating the residual values by regressing out the effects of age, sex, their interaction and intracranial brain volume and (2) for each individual, subtracting the average value for a region and dividing it by the standard deviation calculated from the subjects who were free from neuropsychiatric disorders. This produced a vector of 24 normalized z-values (35 values for gray matter thickness, 7 values for the subcortical volumes) for every individual in the sample. The regularization was performed once and for the entire sample. The individual white matter RVI for MDD and AD was then calculated as the correlation coefficient between 24 region-wise *z* values for the subject and their effect sizes for the MDD-control group differences in ENIGMA. The same procedure was used to generate a cortical thickness based RVI and a subcortical structural volume based RVI. The whole-brain RVI was calculated as the average of the three tissue-specific RVIs. The RVI calculator is distributed with the SOLAR-Eclipse software (www.solar-eclipse-genetics.org).

#### 2.4.2. Group comparison

Analysis of variance (ANOVA) was used to compare group differences for the global and regional cortical, subcortical, and white matter measurements in the UKBB sample, with adjustments for the effects of age and sex. Using a Bonferroni correction to reduce Type I errors associated with multiple comparisons, we set the significance threshold to $p < 0.05/33 = 0.001$ for cortical, $p < 0.05/8 = 0.007$ for subcortical, and $p < 0.05/24 = 0.002$ for white matter measures. All analyses were first performed using the combined patient group and comparing to the controls.

## 3. Results

### 3.1. Neuroimaging measures in neuropsychiatric illnesses

UKBB participants with MDD showed significantly lower whole-brain average FA values (Cohen's $d = -0.10$, t = 4.6, p = $5{\cdot}10^{-5}$) but no detectable difference in whole brain average or regional cortical thickness (Cohen's $d \leq -0.05$, t ≤ 1.5, p > 0.1) or subcortical volumes (Cohen's $d \leq 0.08$, t ≤ 0.92, p > 0.3) compared to controls with no neuropsychiatric conditions. Relative to healthy controls, UKBB participants with AD showed significantly lower average FA values (Cohen's $d = -0.73$, t = 2.6, p = 0.01), average cortical thickness (Cohen's $d = -0.52$, t = 2.4, p = 0.02) and volume deficits in several subcortical structures, with the largest effect on hippocampal volume (Cohen's $d = -1.16$, t = 4.5, p = $7{\cdot}10^{-6}$) compared to the controls.

The combined regional effect sizes for cortical, subcortical and white matter measurements showed strong correlation between UKBB-MDD effect sizes and these reported by the ENIGMA-MDD working group (r = 0.76). The regional effect sizes for MDD were correlated between UKBB and ENIGMA for white matter (r = 0.73) but not for subcortical volume (r = 0.53), or the cortical gray matter thickness (r = 0.27) measurements (Fig. 1A–C).

Combining data across the three modalities, the AD patterns between UKBB and ADNI were moderately correlated (r = 0.51). However, for each of the three modalities, we observed strong correlation among effect sizes between UKBB and ADNI (r = 0.61, 0.70, 0.67) (Fig. 1D–F).

### 3.2. RVI disease specificity: MDD vs. AD

We first examined psychiatric vs. neurological disease specificity using whole-brain, cross-tissue RVI in subjects with two representative diseases: MDD vs. AD. Compared to controls, patients with MDD (N = 2,240) showed significantly elevated whole-brain RVI-MDD (Cohen's $d = 0.15$, t = 5.3, p = $10^{-7}$) but not RVI-AD (Cohen's $d = 0.09$, t = 2.0, p = 0.10) (Fig. 2A vs. C). In comparison, patients with Alzheimer's disease (N = 7) showed significant elevation in whole-brain RVI-AD (Cohen's $d = 1.4$, t = 4.2, p = $10^{-5}$) but not in RVI-MDD (Fig. 2A vs. C). Therefore, despite the large differences in sample sizes, the statistical double-dissociation data suggest some degree of disease specificity of the whole-brain, cross-tissue RVI approach for these two diagnoses.

In specific tissues, white matter ($d = 0.14$, t = 5.5, p = $10^{-7}$) and

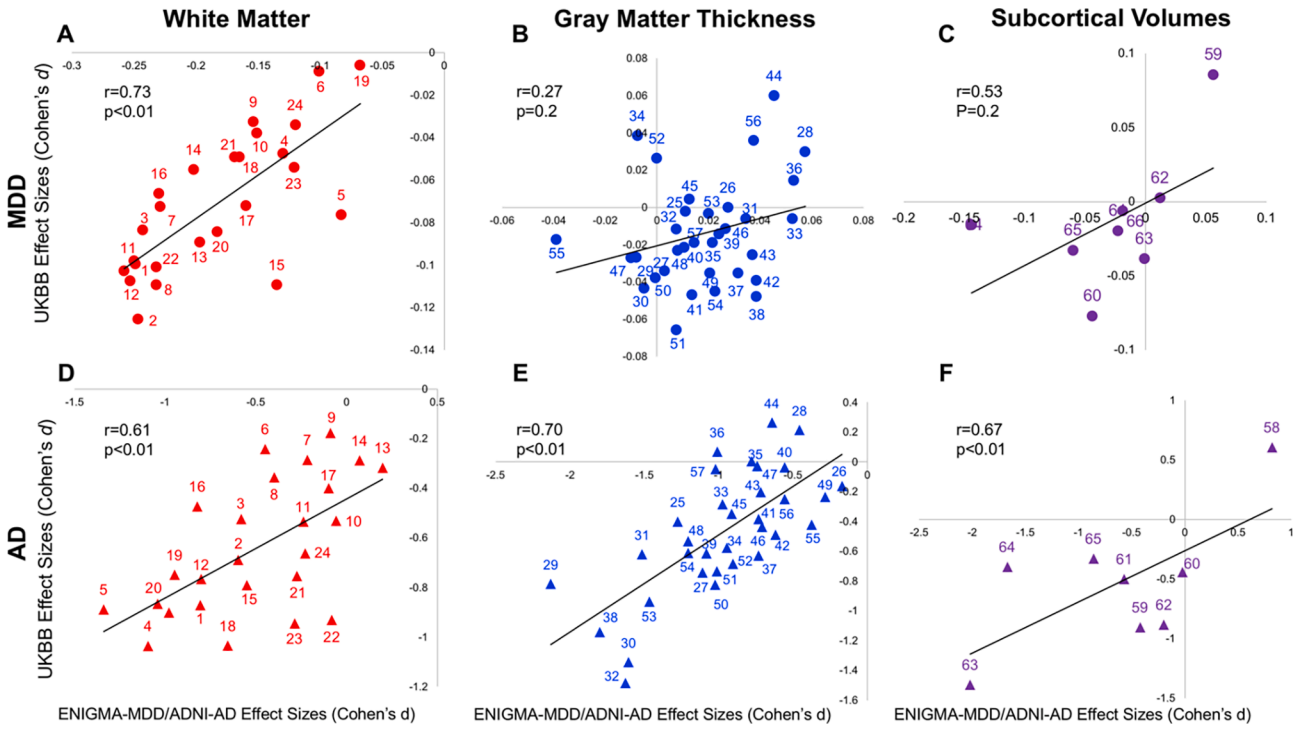


**Fig. 1.** Regional effect sizes (Cohen's d-values) calculated for MDD and AD in UKBB versus effect sizes reported by ENIGMA or ADNI consortium. *White Matter:* 1 Corpus Callosum (CC) 2 Genu of Corpus Callosum (GCC) 3 Body of Corpus Callosum (BCC) 4 Splenium of Corpus Callosum (SCC) 5 Fornix (FX) 6 Cortico-Spinal Tract (CST) 7 Internal Capsule (IC) 8 Anterior Limb of Internal Capsule (ALIC) 9 Posterior Limb of Internal Capsule (PLIC) 10 Retrolenticular Limb of the Internal Capsule (RLIC) 11 Corona Radiata (CR) 12 Anterior Corona Radiata (ACR) 13 Superior Corona Radiata (SCR) 14 Posterior Corona Radiata (PCR) 15 Posterior Thalamic Radiation (PTR) 16 Sagittal Striatum (SS) 17 External Capsule (EC) 18 Cingulum (CGC) 19 Cingulum hippocampus gyrus (CHG) 20 Fornix-Stria Terminalis (FXST) 21 Superior Longitudinal Fasciculus (SLF) 22 Superior Fronto-Occipital Fasciculus (SFO) 23 Uncinate Fasciculus (UNC) 24 Tapetum (TAP) | *Gray Matter Thickness:* 25 Banks of Superior Temporal Sulcus 26 Caudal Anterior Cingulate Cortex, 27 Caudal Middle Frontal Gyrus, 28 Cuneus, 29 Entorhinal Cortex, 30 Fusiform Gyrus, 31 Inferior Parietal Cortex, 32 Inferior Temporal Gyrus, 33 Isthmus Cingulate Cortex, 34 Lateral Occipital Cortex, 35 Lateral Orbitofrontal Cortex 36 Lingual Gyrus 37 Medial Orbitofrontal Cortex 38 Middle Temporal Gyrus 39 Parahippocampal Gyrus 40 Paracentral Lobule 41 Pars Opercularis of Inferior Frontal Gyrus 42 Pars Orbitalis of Inferior Frontal Gyrus 43 Pars Triangularis of Inferior Frontal Gyrus 44 Pericalcarine Cortex 45 Postcentral Gyrus 46 Posterior Cingulate Cortex 47 Precentral Gyrus 48 Precuneus 49 Rostral Anterior Cingulate Cortex 50 Rostral Middle Frontal Gyrus 51 Superior Frontal Gyrus 52 Superior Parietal Cortex 53 Superior Temporal Gyrus 54 Supramarginal Gyrus 55 Frontal Pole 56 Transverse Temporal Gyrus 57 Insula | *Gray Matter Subcortical Volume:* 58 Lateral Ventricle 59 Thalamus 60 Caudate 61 Putamen 62 Palladium 63 Hippocampus 64 Amygdala 65 Accumbens.

subcortical RVI-MDD (Cohen's $d$ = 0.07, t = 2.6, p = 0.009) were significantly elevated in MDD patients compared to controls, while cortical RVI-MDD showed no significant differences (Cohen's $d$ = 0.07, t = 2.0, p = 0.07) (Fig. 2B). None of the tissue specific RVI-MDD values showed significant difference in AD subjects when compared to controls (p = 0.06–0.3) (Fig. 2D).

Patients with AD showed significantly elevated RVI-AD for cortical thickness (Cohen's $d$ = 1.28, t = 3.8, p = $10^{-4}$), subcortical gray matter volume (Cohen's $d$ = 0.81, t = 2.4, p = 0.01), and white matter (Cohen's $d$ = 0.90, t = 2.9, p = 0.003) compared to controls (Fig. 2D). None of the tissue specific RVI-AD values showed significant differences in MDD patients when compared to controls (p = 0.08–0.8) (Fig. 2D). Therefore, although less robust, tissue specific RVI also demonstrated disease specificity between MDD vs. AD.

The MDD patient-control effect size for whole-brain RVI-MDD ($d$ = 0.15) was stronger than the average effect sizes for whole-brain FA ($d$ = −0.10), whole brain average cortical thickness ($d$ = −0.05), and hippocampal volumes ($d$ = −0.02), which showed largest effect size among the subcortical regions. Similarly, the AD patient-control effect size for whole-brain RVI-AD was stronger than the average effect sizes for whole-brain FA, whole brain average cortical thickness and hippocampal volumes: $d$ = 1.4 vs −0.73, −0.52 and −1.16. Furthermore, effect sizes for tissue specific RVIs were numerically larger than those for individual trait measurements.

### 3.3. RVI specificity within major psychiatric illnesses

We compared the elevation of RVI-MDD in MDD to two closely related affected disorders: bipolar and anxiety disorder (Fig. 3A and B). Unlike patients with MDD (t = 5.3, p = $10^{-7}$; same data above), patients with bipolar and anxiety disorders showed no significant elevation in whole-brain RVI-MDD (t = 2.0, p = 0.05 and t = 0.6, p = 0.5, respectively), compared to controls. Therefore, even among affective disorders, whole-brain RVI-MDD demonstrated specificity for MDD, although the separation between MDD and bipolar disorder was limited. The RVI for other psychiatric disorders are unavailable, pending large scale meta-analytical results from ENIGMA.

Exploring effects on specific tissues (Fig. 3B), the white matter RVI-MDD (t = 5.5, p = $10^{-7}$) and subcortical volume RVI-MDD (t = 2.6, p = 0.009) and showed significant elevation in MDD patients compared to controls (same data as above). Participants with bipolar disorder showed elevation in white matter RVI-MDD ($d$ = 0.24, t = 2.7, p = 0.008) but not in cortical thickness or subcortical volume RVI-MDD ($d$ = 0.12, t = 1.4 and $d$ = 0.32, t = 1.9, p = 0.07, respectively). Subjects with anxiety disorder showed no elevation in any tissue specific RVI-MDD, although the elevation in subcortical RVI approached significance (d = 0.09, t = 2.3, p = 0.02). These data suggest that the disease specificity of RVI-MDD can be clearly demonstrated with anxiety disorder, but less effective with bipolar disorder.

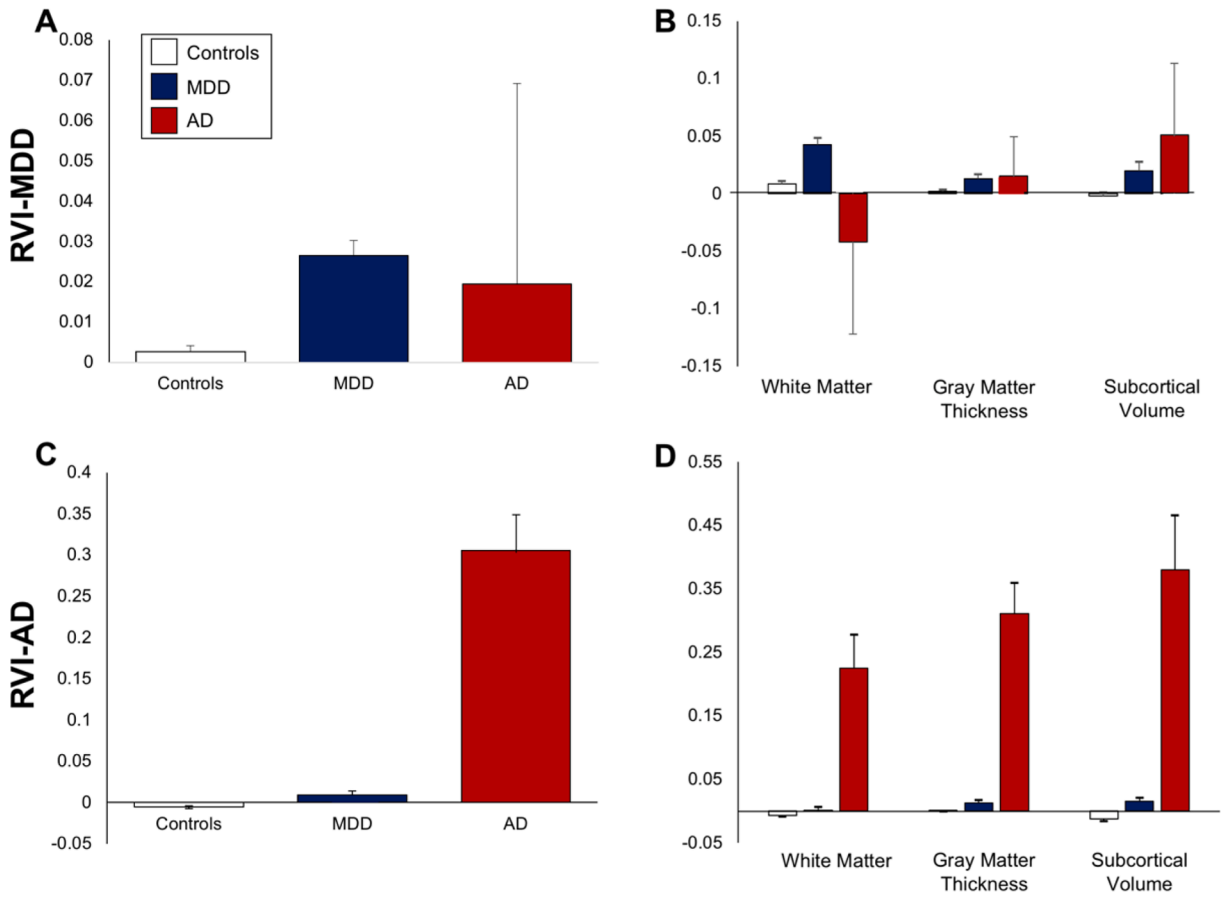


**Fig. 2.** Group comparisons RVI-MDD and RVI-AD measures for controls and subjects with MDD and AD. Whole-brain (panel A and C) and tissue-specific RVI (panel B and D) values for RVI-MDD and RVI-AD, respectively.

### *3.4. RVI specificity within neurological illnesses*

Similarly, we compared disease specificity of RVI-AD among three major neurological disease categories available in the UKBB data: AD (N = 7), PD (N = 37) and stroke (N = 247) (Fig. 3). Whole-brain RVI-AD was elevated in patients with AD ($d = 1.4$, t = 4.2, $p = 10^{-5}$, same data as above), PD ($d = 0.50$, t = 2.4p = 0.004) but not stroke ($d = 0.10$, t = 1.1, p = 0.3) (Fig. 3C).

In specific tissues (Fig. 3D), patients with PD showed significant elevation in RVI-AD for white matter ($d = 0.28$, t = 2.1, p = 0.02) and subcortical gray matter volume ($d = 0.40$, t = 2.4, p = 0.004) but not in cortical thickness ($d = 0.17$, t = 0.6, p = 0.2). Patients with stroke showed a significant elevation in RVI-AD for subcortical gray matter volume ($d = 0.21$, t = 2.7, p = 0.001) but no significant elevation of RVI-AD for white matter ($d = 0.14$, t = −1.5, p = 0.3) or cortical thickness ($d = 0.05$, t = 0.7, p = 0.5). Therefore, whole-brain RVI-AD, but not tissue specific RVI-AD, showed some level of AD specificity, as compared to PD and stroke (Fig. 3C vs. 3D).

## 4. Discussion

Using the largest available epidemiological dataset, we tested replication and sensitivity of the patterns of regional neuroanatomic deficits for major depressive disorder (MDD) and Alzheimer's Disease. The whole-brain deficit patterns showed strong correlation between UKBB and ENIGMA for MDD and between UKBB and ADNI for AD. Tissue specific effect sizes were likewise correlated with an exception for cortical deficits for MDD, where the MDD-control differences were not significant in either the UKBB or ENIGMA samples. The Regional Vulnerability Index (RVI) were significantly elevated in UKBB subjects with MDD and AD in the participants with these respective disorders. The effect sizes for the whole-brain and tissue specific RVI-MDD and AD in patient-control comparisons, were stronger than these for the whole-brain average white matter FA, gray matter thickness and individual subcortical measurements. This suggests that the patterns of similarity to a disorder may be a better predictor of vulnerability than absolute neuroimaging measurements. Testing across disorders showed evidence for specificity and suggested that disorder-specific deficit patterns is a useful biomarker for population-wide assessments of similarity to these neuropsychiatric illnesses.

Big data studies have markedly improved the stability of neuroimaging findings and provided a strong rationale to use meta-analytic signatures of neuropsychiatric disorders as a measure of vulnerability at the individual level (Kochunov et al., 2020a, 2019c). The ENIGMA-MDD workgroup, in particular, has reported regional patterns of white matter, cortical and subcortical deficits in patients by assembling the largest and most inclusive samples to date (Schmaal et al., 2017, 2016; van Velzen et al., 2019). In this study, the MDD deficit patterns derived by these ENIGMA studies showed a strong correlation (r = 0.76) with the patient-control regional effect sizes in the UKBB sample at the whole-brain level. The high effect sizes for white matter, cortical and subcortical deficit patterns observed in ADNI population were like the effect sizes observed in UKBB subjects despite a very small sample (N = 7). The alignment of the whole-brain deficit patterns supports whole-brain RVI for combining measures to assess individual similarity to a disease in terms of its expected neuroanatomical deficit patterns.

The patient-control effect size for whole-brain RVI were stronger than the average effect sizes for whole-brain FA, whole-brain cortical thickness and hippocampal volumes. Similarly, tissue specific RVIs had higher effect sizes than those for individual neuroimaging measures for

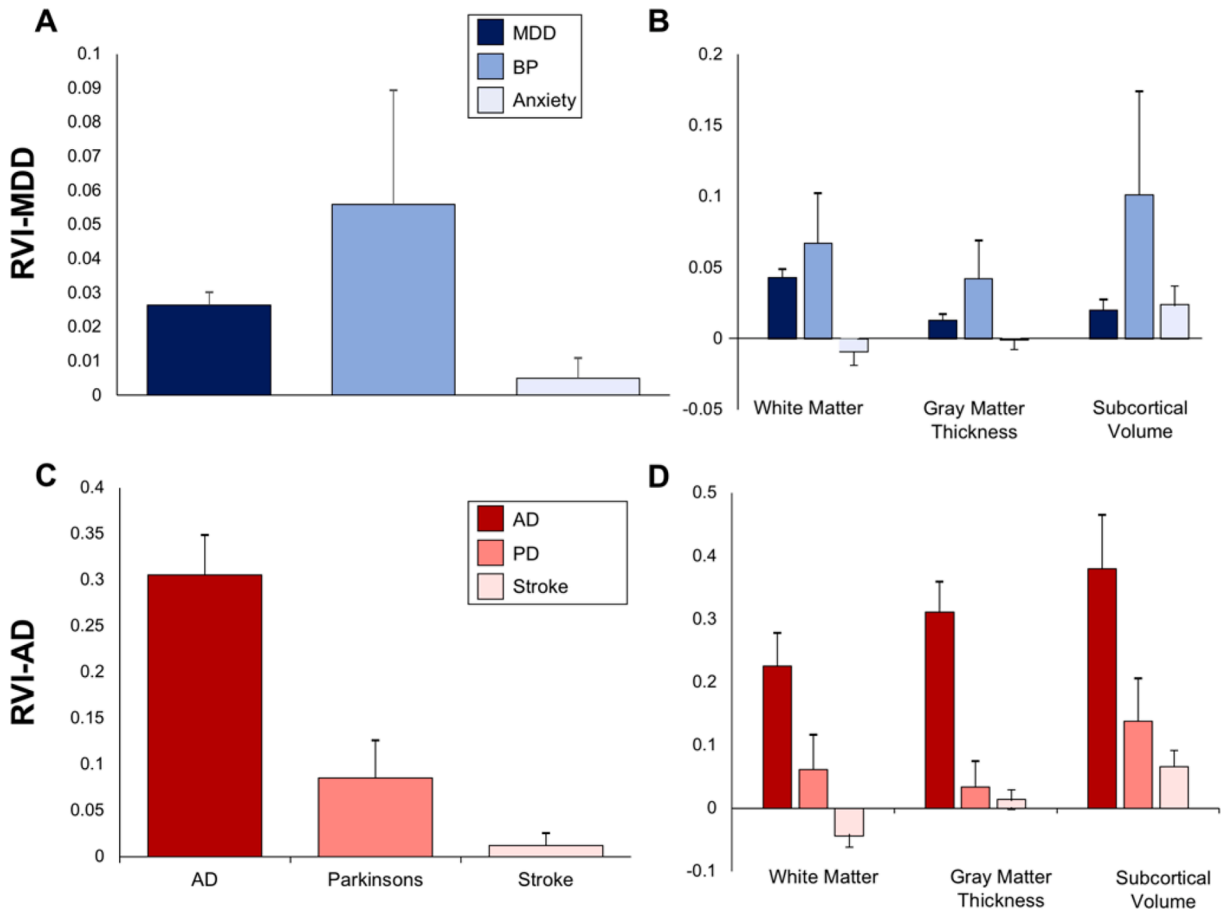


**Fig. 3.** Group comparisons and p-values for whole brain and tissue specific RVI-MDD for subjects with MDD and bipolar disorder (BP) and anxiety disorder (panels A and B). Whole-brain (panel C) and tissues specific (panel D) RVI-AD values for subject with AD, PD and stroke.

the respective domains. RVI is a correlation coefficient between the neuroanatomic regional deficit patterns in an individual and the deficit patterns of a disease. Therefore, RVI is complementary to the individual's regional deficit measurements. The deficit patterns were defined for a specific tissue type and whole-brain, cross-tissue imaging data. RVI is calculated based on regional effect sizes derived by comparing affected subjects with healthy controls. Whether the data generated can be used to compare RVI between two diseases is unclear and limits the statistical comparison of RVIs between two illnesses. Another limitation is that whole brain RVI calculations require the availability of the regional effect sizes across the three tissue types. Among the illnesses discussed in this study, only MDD in ENIGMA and AD from ADNI have such data presently available, which is one of the reasons that this study is focusing on these two illnesses. Using this approach, the whole-brain RVI-MDD and RVI-AD were significantly elevated only in patients with these respective illnesses when compared to controls free of neuropsychiatric disorders, supporting disease specificity.

We further examined whether the RVI approach can separate not just psychiatric and neurological diseases, but also other illnesses within psychiatric and neurological categories. We calculated RVI-MDD in subjects with bipolar and anxiety disorders, as these are affective disorders with overlapping clinical symptoms. Their diagnostic separation is based on clinical history and interviews and there are no biological metrics that can consistently separate among them. Specificity testing showed no significant elevation in the whole-brain RVI-MDD in patients with bipolar disorders or anxiety disorders. However, participants with bipolar disorder showed significant elevation in the white matter RVI-MDD. This was expected given a prior finding of some overlap ($r = 0.28$) between white matter deficit patterns in these disorders (Kochunov et al., 2020a). There was no significant elevation in cortical or subcortical RVI-MDD in participants with bipolar disorder and no significant elevation of any tissue specific RVI-MDD in participants with anxiety disorders. This suggests that the regional deficit patterns in anxiety disorders, and to a lesser extent bipolar disorder, were not as closely aligned with MDD despite similarity in symptoms. This also supports the potential use of RVI or RVI-like approaches for cross-diagnostic research, objective diagnostic differentiation and unique and shared anatomic deficit patterns.

Evaluation of RVI-AD in two other aging-related neurological disorders showed that participants with Parkinson's disease (PD) showed significant elevation in the whole-brain RVI-AD, although at about half of the effect size as in participants with AD. Participants with stroke did not show significantly elevated RVI-AD. Participants with AD showed highly significant elevation in all three tissue-specific RVI with the largest effects observed for subcortical RVI, followed by cortical and white matter RVI, in line with the significant structural alterations in brains of subjects with AD. Subjects with PD showed elevation in the whole brain RVI-AD as well as the RVI-AD values for the white matter and subcortical patterns. PD is the most common age-related neurodegenerative brain disorders with up to 80% of patients converging to mild cognitive impairment and then to AD or other type of dementia, especially in the later, more fulminant stage (Aarsland et al., 2017). The risk of this conversion is higher for PD patients with cognitive deficits that show overlap with these for AD (Aarsland et al., 2017). The risks for developing cognitive deficits in patients with PD are linked to the subcortical volume changes including reduction in hippocampus and white matter atrophy (Lanskey et al., 2018). Therefore, we speculate

that the higher RVI-AD indices in this disease may be driven by some of the brain changes in subjects with PD that coincided with changes in AD as captured by the RVI-AD.

Stroke is another aging-related neurological disorder associated with an elevated risk for AD (Garcia-Alloza et al., 2011; Honig et al., 2003; Kalaria et al., 2008; Luchsinger et al., 2005). We observed widespread regional deficits in cerebral white matter and significantly lower subcortical volumes in subjects with stroke (Table S1). However, there was no significant elevation in RVI-AD white matter or cortical values and only a slight elevation (Cohen's $d = 0.16$) in subcortical RVI-AD values in subjects with stroke. This shows the specificity of the RVI-AD construct even in subjects who otherwise had significantly reduced cerebral integrity. Stroke is characterized by the variability and heterogeneity of lesions due to the diversity of its risk factors, types, causes, and locations which leads to a significant reduction in overall cerebral integrity. While these patterns do not overlap with those observed in AD, cerebrovascular lesions are risk factors for cognitive deficits and eventual reduction in hippocampal volume (Garcia-Alloza et al., 2011), and is likely contributing to the elevated RVI-AD subcortical measurements. Similarly, AD pathophysiology harbors cerebrovascular damage as one of the hallmarks of the disease, particularly on the microvascular level that may be outside the range of standard detection parameters in clinical practice.

This study has several other limitations. The UKBB is a sample of mainly healthy individuals and has a very small number of subjects with AD and other neurodegenerative illnesses. Our primary aim was to evaluate the elevation of RVI-AD in the MDD sample as the test of specificity between the two disorders. However, given very large effect sizes of AD on cerebral integrity we were able to readily replicate AD patterns in this sample, however, these results lack statistical power. At present, we do not have data to calculate RVI for bipolar and anxiety disorders, PD, or stroke and cannot conduct reciprocal testing of these findings. N = 603 of MDD subjects also reported a comorbid diagnosis of anxiety disorder. Post-hoc analyses excluded these subjects and resulted in similar outcomes. The study is also limited as it is based on the existing UKBB sample which is cross-sectional and much of the UKBB diagnosis data is self-reported and not verified by independent clinical interviews (Bycroft et al., 2018). The UKBB sample is focused on subjects in the 5th to 8th decades of life and the interaction between the diagnosis and aging trajectories for different diagnoses may be reflected in RVI values. These limitations reduced our ability to test the predictive validity of the RVI constructs across the major psychiatric vs. neurological conditions. Expansion of these large data sets into different phases of life as well as different phases of disease would allow for improvement upon this validity. With longitudinal data of at-risk populations, development and testing of these findings can be more broadly applied with diagnostic and even causal linkages.

## 5. Conclusion

We used big data-derived deficit patterns to measure similarity between the brain structural and microstructural patterns in an individual and the expected patterns in MDD and AD as calculated by the regional vulnerability index (RVI) for each disease. We tested the utility of RVI-based phenotypes for assessing individual resemblance to distinct (AD vs. MDD) vs. similar mood psychiatric (bipolar disorder, anxiety) and aging-related neurological (PD, stroke) diseases. The results demonstrated that the RVI-derived disease markers may be replicable across big data samples and can reasonably differentiate across categories of diseases, especially when effects across different tissue types are considered. These findings encourage longitudinal studies, especially studies of prodromal subjects and across a broader range of diseases, to test the predictive validity to RVI as a vulnerability index.

## Funding

This work was supported by the National Institutes of Health grants R01MH112180, R01MH116948, S10OD023696, R01EB015611, R01MH117601, R01AG095874, and U01MH108148. These funding sources provided financial support to enable design and conduct of the study or collection, management, or analysis of the data. LS is supported by a NHMRC Career Development Fellowship (1140764) and a University of Melbourne Dame Kate Campbell fellowship. None of the funding agencies had a role in the interpretation of the data. None had a role in the preparation, review, or approval of the manuscript. None had a role in the decision to submit the manuscript for publication.

## CRediT authorship contribution statement

**Peter Kochunov:** Conceptualization, Data curation, Formal analysis, Funding acquisition, Supervision, Writing - original draft, Writing - review & editing. **Meghann C. Ryan:** Conceptualization, Data curation, Formal analysis, Writing - review & editing. **Qifan Yang:** Conceptualization, Data curation, Writing - original draft, Writing - review & editing. **Kathryn S. Hatch:** Conceptualization, Data curation, Writing - original draft, Writing - review & editing. **Alyssa Zhu:** Conceptualization, Data curation, Writing - original draft, Writing - review & editing. **Sophia I. Thomopoulos:** Conceptualization, Data curation. **Neda Jahanshad:** Conceptualization, Funding acquisition, Writing - review & editing. **Lianne Schmaal:** Writing - review & editing. **Paul M. Thompson:** Funding acquisition, Supervision, Writing - original draft, Writing - review & editing. **Shuo Chen:** Writing - review & editing. **Xiaoming Du:** Writing - review & editing. **Bhim M. Adhikari:** Writing - review & editing. **Heather Bruce:** Writing - review & editing. **Stephanie Hare:** Writing - review & editing. **Eric L. Goldwaser:** Writing - review & editing. **Mark D. Kvarta:** Writing - review & editing. **Thomas E. Nichols:** Funding acquisition, Writing - review & editing. **L. Elliot Hong:** Funding acquisition, Supervision, Writing - original draft, Writing - review & editing.

## Declaration of Competing Interest

LEH has received or plans to receive research funding or consulting fees on research projects from Mitsubishi, Your Energy Systems LLC, Neuralstem, Taisho, Heptares, Pfizer, Luye Pharma, Sound Pharma, Takeda, and Regeneron. None was involved in the design, analysis or outcomes of the study. Paul Thompson and Neda Jahanshad received grant support from Biogen, Inc. (Boston, USA) for research unrelated to the topic of this manuscript. All other authors declare no conflicts of interest.

## Appendix A. Supplementary data

Supplementary data to this article can be found online at https://doi.org/10.1016/j.nicl.2021.102574.

## References

Aarsland, D., Creese, B., Politis, M., Chaudhuri, K.R., Ffytche, D.H., Weintraub, D., Ballard, C., 2017. Cognitive decline in Parkinson disease. Nat. Rev. Neurol. 13, 217–231.

Bycroft, C., Freeman, C., Petkova, D., Band, G., Elliott, L.T., Sharp, K., Motyer, A., Vukcevic, D., Delaneau, O., O'Connell, J., Cortes, A., Welsh, S., Young, A., Effingham, M., McVean, G., Leslie, S., Allen, N., Donnelly, P., Marchini, J., 2018. The UK Biobank resource with deep phenotyping and genomic data. Nature 562, 203–209.

Garcia-Alloza, M., Gregory, J., Kuchibhotla, K.V., Fine, S., Wei, Y., Ayata, C., Frosch, M. P., Greenberg, S.M., Bacskai, B.J., 2011. Cerebrovascular lesions induce transient beta-amyloid deposition. Brain 134, 3697–3707.

Heresco-Levy, U., Ermilov, M., Shimoni, J., Shapira, B., Silipo, G., Javitt, D.C., 2002. Placebo-controlled trial of D-cycloserine added to conventional neuroleptics, olanzapine, or risperidone in schizophrenia. Am. J. Psychiatry 159, 480–482.

Hoffman, R.E., Hawkins, K.A., Gueorguieva, R., Boutros, N.N., Rachid, F., Carroll, K., Krystal, J.H., 2003. Transcranial magnetic stimulation of left temporoparietal cortex and medication-resistant auditory hallucinations. Arch. Gen. Psychiatry 60, 49–56.

Honig, L.S., Tang, M.-X., Albert, S., Costa, R., Luchsinger, J., Manly, J., Stern, Y., Mayeux, R., 2003. Stroke and the Risk of Alzheimer Disease. Arch. Neurol. 60, 1707–1712.

Kalaria, R.N., Maestre, G.E., Arizaga, R., Friedland, R.P., Galasko, D., Hall, K., Luchsinger, J.A., Ogunniyi, A., Perry, E.K., Potocnik, F., Prince, M., Stewart, R., Wimo, A., Zhang, Z.X., Antuono, P., World Federation of Neurology Dementia Research, G., 2008. Alzheimer's disease and vascular dementia in developing countries: prevalence, management, and risk factors. Lancet Neurol. 7, 812–826.

Kane, J., Honigfeld, G., Singer, J., Meltzer, H., 1988. Clozapine for the treatment-resistant schizophrenic. A double-blind comparison with chlorpromazine. Arch. Gen. Psychiatry 45, 789–796.

Kelly, S., Jahanshad, N., Zalesky, A., Kochunov, P., Agartz, I., Alloza, C., Andreassen, O. A., Arango, C., Banaj, N., Bouix, S., Bousman, C.A., Brouwer, R.M., Bruggemann, J., Bustillo, J., Cahn, W., Calhoun, V., Cannon, D., Carr, V., Catts, S., Chen, J., Chen, J. X., Chen, X., Chiapponi, C., Cho, K.K., Ciullo, V., Corvin, A.S., Crespo-Facorro, B., Cropley, V., De Rossi, P., Diaz-Caneja, C.M., Dickie, E.W., Ehrlich, S., Fan, F.M., Faskowitz, J., Fatouros-Bergman, H., Flyckt, L., Ford, J.M., Fouche, J.P., Fukunaga, M., Gill, M., Glahn, D.C., Gollub, R., Goudzwaard, E.D., Guo, H., Gur, R. E., Gur, R.C., Gurholt, T.P., Hashimoto, R., Hatton, S.N., Henskens, F.A., Hibar, D.P., Hickie, I.B., Hong, L.E., Horacek, J., Howells, F.M., Hulshoff Pol, H.E., Hyde, C.L., Isaev, D., Jablensky, A., Jansen, P.R., Janssen, J., Jonsson, E.G., Jung, L.A., Kahn, R. S., Kikinis, Z., Liu, K., Klauser, P., Knochel, C., Kubicki, M., Lagopoulos, J., Langen, C., Lawrie, S., Lenroot, R.K., Lim, K.O., Lopez-Jaramillo, C., Lyall, A., Magnotta, V., Mandl, R.C.W., Mathalon, D.H., McCarley, R.W., McCarthy-Jones, S., McDonald, C., McEwen, S., McIntosh, A., Melicher, T., Mesholam-Gately, R.I., Michie, P.T., Mowry, B., Mueller, B.A., Newell, D.T., O'Donnell, P., Oertel-Knochel, V., Oestreich, L., Paciga, S.A., Pantelis, C., Pasternak, O., Pearlson, G., Pellicano, G.R., Pereira, A., Pineda Zapata, J., Piras, F., Potkin, S.G., Preda, A., Rasser, P.E., Roalf, D.R., Roiz, R., Roos, A., Rotenberg, D., Satterthwaite, T.D., Savadjiev, P., Schall, U., Scott, R.J., Seal, M.L., Seidman, L.J., Shannon Weickert, C., Whelan, C.D., Shenton, M.E., Kwon, J.S., Spalletta, G., Spaniel, F., Sprooten, E., Stablein, M., Stein, D.J., Sundram, S., Tan, Y., Tan, S., Tang, S., Temmingh, H.S., Westlye, L.T., Tonnesen, S., Tordesillas-Gutierrez, D., Doan, N.T., Vaidya, J., van Haren, N.E.M., Vargas, C.D., Vecchio, D., Velakoulis, D., Voineskos, A., Voyvodic, J. Q., Wang, Z., Wan, P., Wei, D., Weickert, T.W., Whalley, H., White, T., Whitford, T. J., Wojcik, J.D., Xiang, H., Xie, Z., Yamamori, H., Yang, F., Yao, N., Zhang, G., Zhao, J., van Erp, T.G.M., Turner, J., Thompson, P.M., Donohoe, G., 2018. Widespread white matter microstructural differences in schizophrenia across 4322 individuals: results from the ENIGMA Schizophrenia DTI Working Group. Mol. Psychiatry 23, 1261–1269.

Kochunov, P., Hong, L.E., 2014. Neurodevelopmental and neurodegenerative models of schizophrenia: white matter at the center stage. Schizophr. Bull. 40, 721–728.

Kochunov, P., Hong, L.E., Dennis, E.L., Morey, R.A., Tate, D.F., Wilde, E.A., Logue, M., Kelly, S., Donohoe, G., Favre, P., Houenou, J., Ching, C.R.K., Holleran, L., Andreassen, O.A., van Velzen, L.S., Schmaal, L., Villalon-Reina, J.E., Bearden, C.E., Piras, F., Spalletta, G., van den Heuvel, O.A., Veltman, D.J., Stein, D.J., Ryan, M.C., Tan, Y., van Erp, T.G.M., Turner, J.A., Haddad, L., Nir, T.M., Glahn, D.C., Thompson, P.M., Jahanshad, N., 2020a. ENIGMA-DTI: Translating reproducible white matter deficits into personalized vulnerability metrics in cross-diagnostic psychiatric research. Hum Brain Mapp.

Kochunov, P., Huang, J., Chen, S., Li, Y., Tan, S., Fan, F., Feng, W., Wang, Y., Rowland, L., Savransky, A., Du, X., Chiappelli, J., Chen, S., Jahanshad, N., Thompson, P.M., Ryan, M.C., Adhikari, B., Sampath, H., Cui, Y., Wang, Z., Yang, F., Tan, Y., Hong, L.E., 2019a. White matter in schizophrenia treatment resistance. Am. J. Psychiatry 176, 829–838.

Kochunov, P., Veraart, J., Jahanshad, N., Eskandar, G., Du, X., Muellerklein, F., Savransky, A., Shukla, D., Sampath, H., Thompson, P.M., 2016. Diffusion-weighted imaging uncovers likely sources of processing-speed deficits in schizophrenia. Proc. Natl. Acad. Sci. U.S.A. 113, 13504–13509.

Kochunov, P., Thompson, P.M., Hong, L.E., 2019b. Toward high reproducibility and accountable heterogeneity in schizophrenia research. JAMA Psychiatry 76, 680–681.

Kochunov, P., Thompson, P.M., Hong, L.E., 2019c. Toward high reproducibility and accountable heterogeneity in schizophrenia researchtoward high reproducibility and accountable heterogeneity in schizophrenia. JAMA Psychiatry.

Kochunov, P., Zavaliangos-Petropulli, A., Jahandshad, N., Thompson, P.M., Ryan, M.C., Chiappelli, J., Chen, S., Du, X., Hatch, K.S., Adhikari, B.M., Sampath, H., Hare, S., Kvarta, M., Goldwaser, E., Yang, E., Olvera, R.L., Fox, P.T., Curran, J.E., Blangero, J., Glahn, D.C., Tan, Y., Hong, L.E., 2020b. A White Matter Connection of Schizophrenia and Alzheimer's Disease Schizophrenia Bulletin In Press.

Kulkarni, J., Gavrilidis, E., Wang, W., Worsley, R., Fitzgerald, P.B., Gurvich, C., Van Rheenen, T., Berk, M., Burger, H., 2015. Estradiol for treatment-resistant schizophrenia: a large-scale randomized-controlled trial in women of child-bearing age. Mol. Psychiatry 20, 695–702.

Lanskey, J.H., McColgan, P., Schrag, A.E., Acosta-Cabronero, J., Rees, G., Morris, H.R., Weil, R.S., 2018. Can neuroimaging predict dementia in Parkinson's disease? Brain 141, 2545–2560.

Luchsinger, J.A., Reitz, C., Honig, L.S., Tang, M.X., Shea, S., Mayeux, R., 2005. Aggregation of vascular risk factors and risk of incident Alzheimer disease. Neurology 65, 545–551.

Manolio, T.A., Weis, B.K., Cowie, C.C., Hoover, R.N., Hudson, K., Kramer, B.S., Berg, C., Collins, R., Ewart, W., Gaziano, J.M., Hirschfeld, S., Marcus, P.M., Masys, D., McCarty, C.A., McLaughlin, J., Patel, A.V., Peakman, T., Pedersen, N.L., Schaefer, C., Scott, J.A., Sprosen, T., Walport, M., Collins, F.S., 2012. New models for large prospective studies: is there a better way? Am. J. Epidemiol. 175, 859–866.

Samara, M.T., Dold, M., Gianatsi, M., Nikolakopoulou, A., Helfer, B., Salanti, G., Leucht, S., 2016. Efficacy, acceptability, and tolerability of antipsychotics in treatment-resistant schizophrenia: a network meta-analysis. JAMA Psychiatry 73, 199–210.

Schmaal, L., Hibar, D.P., Samann, P.G., Hall, G.B., Baune, B.T., Jahanshad, N., Cheung, J. W., van Erp, T.G.M., Bos, D., Ikram, M.A., Vernooij, M.W., Niessen, W.J., Tiemeier, H., Hofman, A., Wittfeld, K., Grabe, H.J., Janowitz, D., Bulow, R., Selonke, M., Volzke, H., Grotegerd, D., Dannlowski, U., Arolt, V., Opel, N., Heindel, W., Kugel, H., Hoehn, D., Czisch, M., Couvy-Duchesne, B., Renteria, M.E., Strike, L.T., Wright, M.J., Mills, N.T., de Zubicaray, G.I., McMahon, K.L., Medland, S. E., Martin, N.G., Gillespie, N.A., Goya-Maldonado, R., Gruber, O., Kramer, B., Hatton, S.N., Lagopoulos, J., Hickie, I.B., Frodl, T., Carballedo, A., Frey, E.M., van Velzen, L.S., Penninx, B., van Tol, M.J., van der Wee, N.J., Davey, C.G., Harrison, B. J., Mwangi, B., Cao, B., Soares, J.C., Veer, I.M., Walter, H., Schoepf, D., Zurowski, B., Konrad, C., Schramm, E., Normann, C., Schnell, K., Sacchet, M.D., Gotlib, I.H., MacQueen, G.M., Godlewska, B.R., Nickson, T., McIntosh, A.M., Papmeyer, M., Whalley, H.C., Hall, J., Sussmann, J.E., Li, M., Walter, M., Aftanas, L., Brack, I., Bokhan, N.A., Thompson, P.M., Veltman, D.J., 2017. Cortical abnormalities in adults and adolescents with major depression based on brain scans from 20 cohorts worldwide in the ENIGMA Major Depressive Disorder Working Group. Mol. Psychiatry 22, 900–909.

Schmaal, L., Veltman, D.J., van Erp, T.G., Samann, P.G., Frodl, T., Jahanshad, N., Loehrer, E., Tiemeier, H., Hofman, A., Niessen, W.J., Vernooij, M.W., Ikram, M.A., Wittfeld, K., Grabe, H.J., Block, A., Hegenscheid, K., Volzke, H., Hoehn, D., Czisch, M., Lagopoulos, J., Hatton, S.N., Hickie, I.B., Goya-Maldonado, R., Kramer, B., Gruber, O., Couvy-Duchesne, B., Renteria, M.E., Strike, L.T., Mills, N.T., de Zubicaray, G.I., McMahon, K.L., Medland, S.E., Martin, N.G., Gillespie, N.A., Wright, M.J., Hall, G.B., MacQueen, G.M., Frey, E.M., Carballedo, A., van Velzen, L. S., van Tol, M.J., van der Wee, N.J., Veer, I.M., Walter, H., Schnell, K., Schramm, E., Normann, C., Schoepf, D., Konrad, C., Zurowski, B., Nickson, T., McIntosh, A.M., Papmeyer, M., Whalley, H.C., Sussmann, J.E., Godlewska, B.R., Cowen, P.J., Fischer, F.H., Rose, M., Penninx, B.W., Thompson, P.M., Hibar, D.P., 2016. Subcortical brain alterations in major depressive disorder: findings from the ENIGMA Major Depressive Disorder working group. Mol. Psychiatry 21, 806–812.

Thompson, P.M., Andreassen, O.A., Arias-Vasquez, A., Bearden, C.E., Boedhoe, P.S., Brouwer, R.M., Buckner, R.L., Buitelaar, J.K., Bulayeva, K.B., Cannon, D.M., Cohen, R.A., Conrod, P.J., Dale, A.M., Deary, I.J., Dennis, E.L., de Reus, M.A., Desrivieres, S., Dima, D., Donohoe, G., Fisher, S.E., Fouche, J.P., Francks, C., Frangou, S., Franke, B., Ganjgahi, H., Garavan, H., Glahn, D.C., Grabe, H.J., Guadalupe, T., Gutman, B.A., Hashimoto, R., Hibar, D.P., Holland, D., Hoogman, M., Pol, H.E.H., Hosten, N., Jahanshad, N., Kelly, S., Kochunov, P., Kremen, W.S., Lee, P. H., Mackey, S., Martin, N.G., Mazoyer, B., McDonald, C., Medland, S.E., Morey, R.A., Nichols, T.E., Paus, T., Pausova, Z., Schmaal, L., Schumann, G., Shen, L., Sisodiya, S. M., Smit, D.J.A., Smoller, J.W., Stein, D.J., Stein, J.L., Toro, R., Turner, J.A., van den Heuvel, M.P., van den Heuvel, O.L., van Erp, T.G.M., van Rooij, D., Veltman, D.J., Walter, H., Wang, Y., Wardlaw, J.M., Whelan, C.D., Wright, M.J., Ye, J., Consortium, E., 2017. ENIGMA and the individual: predicting factors that affect the brain in 35 countries worldwide. Neuroimage 145, 389–408.

Thompson, P.M., Jahanshad, N., Ching, C.R.K., Salminen, L.E., Thomopoulos, S.I., Bright, J., Baune, B.T., Bertolin, S., Bralten, J., Bruin, W.B., Bulow, R., Chen, J., Chye, Y., Dannlowski, U., de Kovel, C.G.F., Donohoe, G., Eyler, L.T., Faraone, S.V., Favre, P., Filippi, C.A., Frodl, T., Garijo, D., Gil, Y., Grabe, H.J., Grasby, K.L., Hajek, T., Han, L.K.M., Hatton, S.N., Hilbert, K., Ho, T.C., Holleran, L., Homuth, G., Hosten, N., Houenou, J., Ivanov, I., Jia, T., Kelly, S., Klein, M., Kwon, J.S., Laansma, M.A., Leerssen, J., Lueken, U., Nunes, A., Neill, J.O., Opel, N., Piras, F., Piras, F., Postema, M.C., Pozzi, E., Shatokhina, N., Soriano-Mas, C., Spalletta, G., Sun, D., Teumer, A., Tilot, A.K., Tozzi, L., van der Merwe, C., Van Someren, E.J.W., van Wingen, G.A., Volzke, H., Walton, E., Wang, L., Winkler, A.M., Wittfeld, K., Wright, M.J., Yun, J.Y., Zhang, G., Zhang-James, Y., Adhikari, B.M., Agartz, I., Aghajani, M., Aleman, A., Althoff, R.R., Altmann, A., Andreassen, O.A., Baron, D.A., Bartnik-Olson, B.L., Marie Bas-Hoogendam, J., Baskin-Sommers, A.R., Bearden, C.E., Berner, L.A., Boedhoe, P.S.W., Brouwer, R.M., Buitelaar, J.K., Caeyenberghs, K., Cecil, C.A.M., Cohen, R.A., Cole, J.H., Conrod, P.J., De Brito, S.A., de Zwarte, S.M.C., Dennis, E.L., Desrivieres, S., Dima, D., Ehrlich, S., Esopenko, C., Fairchild, G., Fisher, S.E., Fouche, J.P., Francks, C., Frangou, S., Franke, B., Garavan, H.P., Glahn, D.C., Groenewold, N.A., Gurholt, T.P., Gutman, B.A., Hahn, T., Harding, I.H., Hernaus, D., Hibar, D.P., Hillary, F.G., Hoogman, M., Hulshoff Pol, H.E., Jalbrzikowski, M., Karkashadze, G.A., Klapwijk, E.T., Knickmeyer, R.C., Kochunov, P., Koerte, I.K., Kong, X.Z., Liew, S.L., Lin, A.P., Logue, M.W., Luders, E., Macciardi, F., Mackey, S., Mayer, A.R., McDonald, C.R., McMahon, A.B., Medland, S. E., Modinos, G., Morey, R.A., Mueller, S.C., Mukherjee, P., Namazova-Baranova, L., Nir, T.M., Olsen, A., Paschou, P., Pine, D.S., Pizzagalli, F., Renteria, M.E., Rohrer, J. D., Samann, P.G., Schmaal, L., Schumann, G., Shiroishi, M.S., Sisodiya, S.M., Smit, D. J.A., Sonderby, I.E., Stein, D.J., Stein, J.L., Tahmasian, M., Tate, D.F., Turner, J.A., van den Heuvel, O.A., van der Wee, N.J.A., van der Werf, Y.D., van Erp, T.G.M., van Haren, N.E.M., van Rooij, D., van Velzen, L.S., Veer, I.M., Veltman, D.J., Villalon-Reina, J.E., Walter, H., Whelan, C.D., Wilde, E.A., Zarei, M., Zelman, V., Consortium, E., 2020. ENIGMA and global neuroscience: a decade of large-scale studies of the brain in health and disease across more than 40 countries. Transl. Psychiatry 10, 100.

van Erp, T.G.M., Hibar, D.P., Rasmussen, J.M., Glahn, D.C., Pearlson, G.D., Andreassen, O.A., Agartz, I., Westlye, L.T., Haukvik, U.K., Dale, A.M., Melle, I., Hartberg, C.B., Gruber, O., Kraemer, B., Zilles, D., Donohoe, G., Kelly, S., McDonald, C., Morris, D.W., Cannon, D.M., Corvin, A., Machielsen, M.W.J.,

Koenders, L., de Haan, L., Veltman, D.J., Satterthwaite, T.D., Wolf, D.H., Gur, R.C., Gur, R.E., Potkin, S.G., Mathalon, D.H., Mueller, B.A., Preda, A., Macciardi, F., Ehrlich, S., Walton, E., Hass, J., Calhoun, V.D., Bockholt, H.J., Sponheim, S.R., Shoemaker, J.M., van Haren, N.E.M., Pol, H.E.H., Ophoff, R.A., Kahn, R.S., Roiz-Santiaez, R., Crespo-Facorro, B., Wang, L., Alpert, K.I., Jansson, E.G., Dimitrova, R., Bois, C., Whalley, H.C., McIntosh, A.M., Lawrie, S.M., Hashimoto, R., Thompson, P. M., Turner, J.A., 2016. Subcortical brain volume abnormalities in 2028 individuals with schizophrenia and 2540 healthy controls via the ENIGMA consortium. Mol. Psychiatry 21, 585.

van Erp, T.G.M., Walton, E., Hibar, D.P., Schmaal, L., Jiang, W.H., Glahn, D.C., Pearlson, G.D., Yao, N.L., Fukunaga, M., Hashimoto, R., Okada, N., Yamamori, H., Bustillo, J.R., Clark, V.P., Agartz, I., Mueller, B.A., Cahn, W., de Zwarte, S.M.C., Pol, H.E.H., Kahn, R.S., Ophoff, R.A., van Haren, N.E.M., Andreassen, O.A., Dale, A. M., Doan, N.T., Gurholt, T.P., Hartberg, C.B., Haukvik, U.K., Jorgensen, K.N., Lagerberg, T.V., Melle, I., Westlye, L.T., Gruber, O., Kraemer, B., Richter, A., Zilles, D., Calhoun, V.D., Crespo-Facorro, B., Roiz-Santianez, R., Tordesillas-Gutierrez, D., Loughland, C., Carr, V.J., Catts, S., Cropley, V.L., Fullerton, J.M., Green, M.J., Henskens, F.A., Jablensky, A., Lenroot, R.K., Mowry, B.J., Michie, P.T., Pantelis, C., Quide, Y., Schall, U., Scott, R.J., Cairns, M.J., Seal, M., Tooney, P.A., Rasser, P.E., Cooper, G., Weickert, C.S., Weickert, T.W., Morris, D.W., Hong, E., Kochunov, P., Beard, L.M., Gur, R.E., Gur, R.C., Satterthwaite, T.D., Wolf, D.H., Belger, A., Brown, G.G., Ford, J.M., Macciardi, F., Mathalon, D.H., O'Leary, D.S., Potkin, S.G., Preda, A., Voyvodic, J., Lim, K.O., McEwen, S., Yang, F.D., Tan, Y.L., Tan, S.P., Wang, Z.R., Fan, F.M., Chen, J.X., Xiang, H., Tang, S.Y., Guo, H., Wan, P., Wei, D., Bockholt, H.J., Ehrlich, S., Wolthusen, R.P.F., King, M.D., Shoemaker, J.M., Sponheim, S.R., De Haan, L., Koenders, L., Machielsen, M.W., van Amelsvoort, T., Veltman, D.J., Assogna, F., Banaj, N., de Rossi, P., Iorio, M., Piras, F., Spalletta, G., McKenna, P.J., Pomarol-Clotet, E., Salvador, R., Corvin, A., Donohoe, G., Kelly, S., Whelan, C.D., Dickie, E.W., Rotenberg, D., Voineskos, A.N., Ciufolini, S., Radua, J., Dazzan, P., Murray, R., Marques, T.R., Simmons, A., Borgwardt, S., Egloff, L., Harrisberger, F., Riecher-Rossler, A., Smieskova, R., Alpert, K.I., Wang, L., Jonsson, E.G., Koops, S., Sommer, I.E.C., Bertolino, A., Bonvino, A., Di Giorgio, A., Neilson, E., Mayer, A.R., Stephen, J.M., Kwon, J.S., Yun, J.Y., Cannon, D.M., McDonald, C., Lebedeva, I., Tomyshev, A.S., Akhadov, T., Kaleda, V., Fatouros-Bergman, H., Flyckt, L., Busatto, G.F., Rosa, P.G.P., Serpa, M.H., Zanetti, M.V., Hoschl, C., Skoch, A., Spaniel, F., Tomecek, D., Hagenaars, S.P., McIntosh, A.M., Whalley, H.C., Lawrie, S.M., Knochel, C., Oertel-Knochel, V., Stablein, M., Howells, F.M., Stein, D.J., Temmingh, H.S., Uhlmann, A., Lopez-Jaramillo, C., Dima, D., McMahon, A., Faskowitz, J.I., Gutman, B.A., Jahanshad, N., Thompson, P. M., Turner, J.A., Project, K.S., 2018. Cortical brain abnormalities in 4474 individuals with schizophrenia and 5098 control subjects via the enhancing neuro imaging genetics through meta analysis (ENIGMA) consortium. Biol. Psychiatry 84, 644–654.

van Velzen, L.S., Kelly, S., Isaev, D., Aleman, A., Aftanas, L.I., Bauer, J., Baune, B.T., Brak, I.V., Carballedo, A., Connolly, C.G., Couvy-Duchesne, B., Cullen, K.R., Danilenko, K.V., Dannlowski, U., Enneking, V., Filimonova, E., Forster, K., Frodl, T., Gotlib, I.H., Groenewold, N.A., Grotegerd, D., Harris, M.A., Hatton, S.N., Hawkins, E. L., Hickie, I.B., Ho, T.C., Jansen, A., Kircher, T., Klimes-Dougan, B., Kochunov, P., Krug, A., Lagopoulos, J., Lee, R., Lett, T.A., Li, M., MacMaster, F.P., Martin, N.G., McIntosh, A.M., McLellan, Q., Meinert, S., Nenadic, I., Osipov, E., Penninx, B., Portella, M.J., Repple, J., Roos, A., Sacchet, M.D., Samann, P.G., Schnell, K., Shen, X., Sim, K., Stein, D.J., van Tol, M.J., Tomyshev, A.S., Tozzi, L., Veer, I.M., Vermeiren, R., Vives-Gilabert, Y., Walter, H., Walter, M., van der Wee, N.J.A., van der Werff, S.J.A., Schreiner, M.W., Whalley, H.C., Wright, M.J., Yang, T.T., Zhu, A., Veltman, D.J., Thompson, P.M., Jahanshad, N., Schmaal, L., 2019. White matter disturbances in major depressive disorder: a coordinated analysis across 20 international cohorts in the ENIGMA MDD working group. Mol. Psychiatry.

Weiner, M.W., Veitch, D.P., Aisen, P.S., Beckett, L.A., Cairns, N.J., Cedarbaum, J., Green, R.C., Harvey, D., Jack, C.R., Jagust, W., Luthman, J., Morris, J.C., Petersen, R. C., Saykin, A.J., Shaw, L., Shen, L., Schwarz, A., Toga, A.W., Trojanowski, J.Q., Alzheimer's Disease Neuroimaging, I., 2015. 2014 Update of the Alzheimer's Disease Neuroimaging Initiative: A review of papers published since its inception. Alzheimers Dement. 11, e1–120.

Weiner, M.W., Veitch, D.P., Aisen, P.S., Beckett, L.A., Cairns, N.J., Green, R.C., Harvey, D., Jack Jr., C.R., Jagust, W., Morris, J.C., Petersen, R.C., Salazar, J., Saykin, A.J., Shaw, L.M., Toga, A.W., Trojanowski, J.Q., Alzheimer's Disease Neuroimaging, I., 2017. The Alzheimer's Disease Neuroimaging Initiative 3: Continued innovation for clinical trial improvement. Alzheimers Dement. 13, 561–571.

Zavaliangos-Petropulu, A., Nir, T.M., Thomopoulos, S.I., Reid, R.I., Bernstein, M.A., Borowski, B., Jack Jr., C.R., Weiner, M.W., Jahanshad, N., Thompson, P.M., 2019. Diffusion MRI indices and their relation to cognitive impairment in brain aging: the updated multi-protocol approach in ADNI3. Front. Neuroinform. 13, 2.